Yeast Cells with an Artificial Mineral Shell: Protection and Modification of Living Cells by Biomimetic Mineralization**

*Ben Wang, Peng Liu, Wenge Jiang, Haihua Pan, Xurong Xu, and Ruikang Tang**

In all living organisms, whether very basic or highly complex, nature provides a multiplicity of materials, architectures, systems and functions.[1–4] A number of unicellular organisms have an outer-surface proteinaceous membrane as a template for biomineralization.[5] The resultant thin mineral layer is a functional covering.[6] For example, the mineral shell can protect an egg from invasion from the exterior, and the diatom has an ornately patterned silicified shell that evolved as mechanical protection. But most cells in nature cannot make their own hard shells. Here we show a strategy to fashion an artificial shell for the yeast cell so that it has extensive protection. Individual *Saccharomyces cerevisiae* (*S. cerevisiae*) cells are coated with a uniform calcium mineral layer by first self-assembly of functional polymers (layer-by-layer technique, LbL) and then in situ mineralization under physiological conditions. The viability of the cells is maintained after the encapsulation. The enclosed cells become inert (stationary phase) and their lifetime can be extended. Furthermore, the mineral shell protects the cell under harsh conditions. The encapsulated *S. cerevisiae* can even survive the attack of the lytic enzyme zymolyase. The shell can also be used as a scaffold for chemical and biological functionalization. For example, *S. cerevisiae* becomes magnetic by the incorporation of Fe_3O_4 nanoparticles in the mineral layer. The present work demonstrates that the artificial shell has a great potential in the storage, protection, delivery, and modification of living cells. Furthermore, insights from systems biology combined with an understanding of the molecular mechanisms of functional shells will facilitate the tailoring of "super cells" through biomimetic mineralization.

As *S. cerevisiae* shares a common life cycle and cell structure with higher eukaryotes,[7] it is a popular and successful model system for understanding eukaryotic biology at the cellular and molecular levels.[8,9] Like most natural cells, *S. cerevisiae* cannot induce spontaneous mineralization on its surface. Figure 1a shows a typical scanning electron microscopy (SEM) image of *S. cerevisiae*. Although the precipitation of calcium phosphate is induced in a supersaturated calcium phosphate solution (concentrations of calcium and phosphate ions are 5.0 mm, ionic strength 0.12 m, and pH 6.8), most reactions do not occur on the cell surface. The surface of *S. cerevisiae* is unchanged during the precipitation and the mineral forms separately (Figure 1b). Although some mineralization can occur on the cell surface, the deposited minerals are not uniform and they cannot form an ideal shell around the cell (Figure 1c). This phenomenon can be explained by the chemical structure of the cell wall of *S. cerevisiae*, which consists mainly of polysaccharides made up of glucose, mannose, and *N*-acetylglucosamine.[10] Such a structure hardly induces the templated crystallization of calcium phosphates, which is caused by the relatively low density of electronic charge. Previous studies have already pointed out that the electronic interaction is a key factor in biomineralization.[11,12] It is generally agreed that proteins that are most active in the mediation of biologically directed mineralization contain regions rich in carboxylates or other charged functional groups.[13,14]

The mineralization skill of living cells can be improved by introducing functional factors onto the cell surface.[15,16] LbL has been applied as a general approach for the fabrication of multicomponent films on solid supports.[17] We used two polyelectrolytes with opposite charges, poly(diallyldimethylammonium chloride) (PDADMAC) and poly(acrylic sodium) (PAA) are used. PAA has a high density of carboxylate groups, which provide the active nucleation sites for calcium minerals. When the adsorbed PAA molecules are on the outermost layer of the yeast cell, the physicochemical properties of the cells are altered significantly.[18] The carboxylate groups migrate toward the water–polymer interface and bind Ca^{2+} ions. Upon contact with calcification solution the reorganized surface induces the heterogeneous nucleation of calcium minerals.[19–21] Besides, it is emphasized the LbL coating does not kill the yeast cells after the immobilization.[22,23]

In situ precipitation of calcium phosphates on the LbL-treated *S. cerevisiae* cell surface dominates the mineral formation, and the cells can be fully enclosed by the mineral phase (Figure 1d). SEM shows that the surface of *S. cerevisiae* typically becomes rough and porous and is covered by numerous flakelike nanocrystals. A large-scale SEM view (Figure 1e) shows that practically all of the treated cells have mineral surfaces. The formation of the mineral shell around *S. cerevisiae* cells is confirmed by transmission electron

[*] B. Wang, P. Liu, W. Jiang, Dr. H. Pan, Dr. X. Xu, Prof. R. Tang
Center for Biomaterials and Biopathways
Department of Chemistry, Zhejiang University
Hangzhou, 310027 (China)
Fax: (+86) 571-8795-3736
E-mail: rtang@zju.edu.cn

Supporting information for this article is available on the WWW under http://www.angewandte.org or from the author.
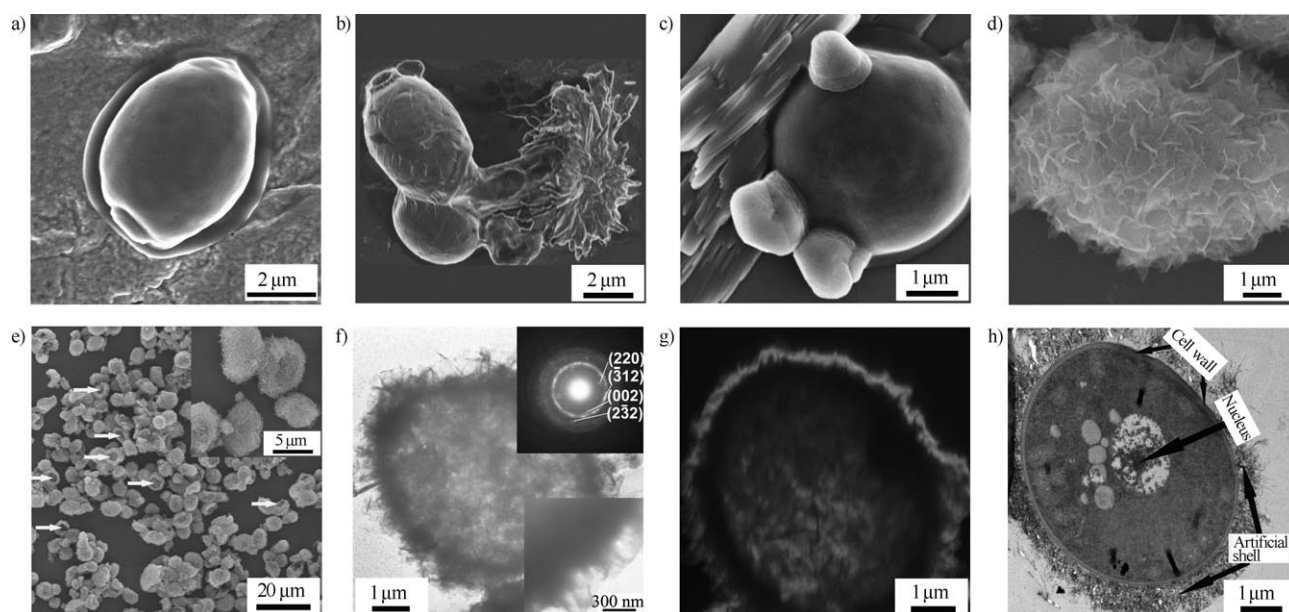
Figure 1. SEM images: a) Bare *S. cerevisiae*. b) *S. cerevisiae* cells are hardly calcified and calcium minerals precipitate separately. c) Some calcium minerals precipitate randomly on the bare cell. d) *S. cerevisiae* with a mineral coat after the LbL treatment. e) A large-scale view of the mineralized cells. f) TEM image of an enclosed *S. cerevisiae* cell; top insert: SAED pattern indicating that the shells contain OCP; bottom insert: enlarged image of the shell. g) Dark-field image showing the OCP phase (bright) around the cell. h) Ultrathin section image of the encapsulated cell.

microscopy (TEM) and selected area electron diffraction (SAED) studies. Figure 1 f shows a typical hollow-structured mineral sphere. The shell consists of two parts, a thin crystallized octacalcium phosphate (OCP) surface and a thick inner layer (700 ± 50 nm). The flakelike nano-OCP crystallites are loosely packed to form the porous surface. The inner layer has a relatively compact structure and is a mixture of OCP and amorphous calcium phosphate (ACP). These mineral phases are confirmed by X-ray diffraction (XRD) and chemical analysis (see Figure S1 in the Supporting Information). Both the bright- and dark-field TEM images (Figure 1 f and 1 g, respectively) imply that the mineral shell has a homogenous and continuous structure, which encases the cell completely. The cell and its mineral shell are clearly distinguished by a cross-section image (Figure 1 h). A similar modification can be obtained by using two other polymers, poly(allylamine hydrochloride) (PAH) and poly(styrene sulfonate) (PSS) (see Figure S2 in the Supporting Information), which suggests that LbL treatment can effectively regulate in situ mineralization on living cells.

It is critical to investigate the physiological behavior of the enclosed cells. By using live–dead viability probes, we find that the viability of these encapsulated cells is maintained. When a culture of mineralized *S. cerevisiae* cells is incubated in a medium containing FUN1 viability indicator and the counterstain Calcofluor White M2R, the metabolically active *S. cerevisiae* processes the FUN1 dye to form red-fluorescent cylindrical structures within their vacuoles. The shift from green to red fluorescence reflects the processing of FUN1 by living cells. Calcofluor White M2R stains the cell walls fluorescent blue, regardless of the metabolic state of *S. cerevisiae*. The calcium phosphate shell is stained by tetracycline hydrochloride, and it exhibits a fluorescent yellow color.

Figure 2 shows that the metabolism of the cells remains in the mineral shell so that they are indeed alive. Again, the shell–wall–vacuole structure is confirmed by the fluorescence study.

The typical life cycle of *S. cerevisiae* is shown in Figure 3 a. Eukaryotic cell proliferation is controlled by specific growth factors and the availability of essential nutrients. If either of these signals is lacking, cells enter into a specialized non-
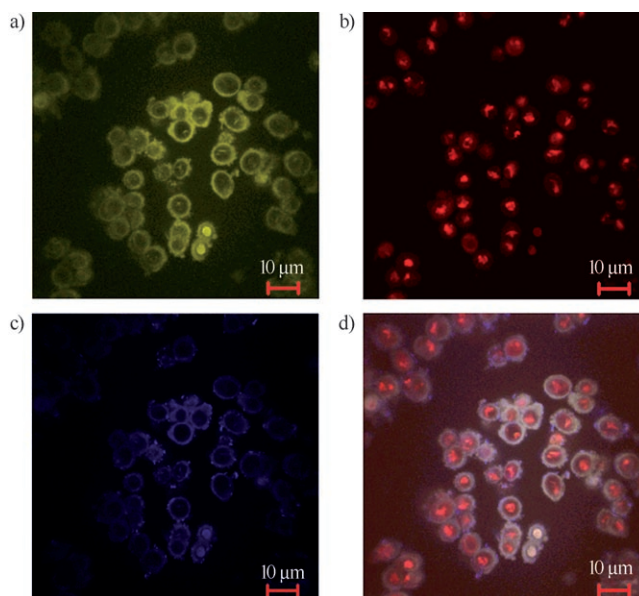
Figure 2. Confocal microscopy images of the fluorescent probes testing for *S. cerevisiae* viability and its mineral shell. a) Mineral shell stained by tetracycline hydrochloride. b) Red spots imply that the cells are alive. c) Cell walls are stained fluorescent blue. d) Combination of the above fluorescence results.
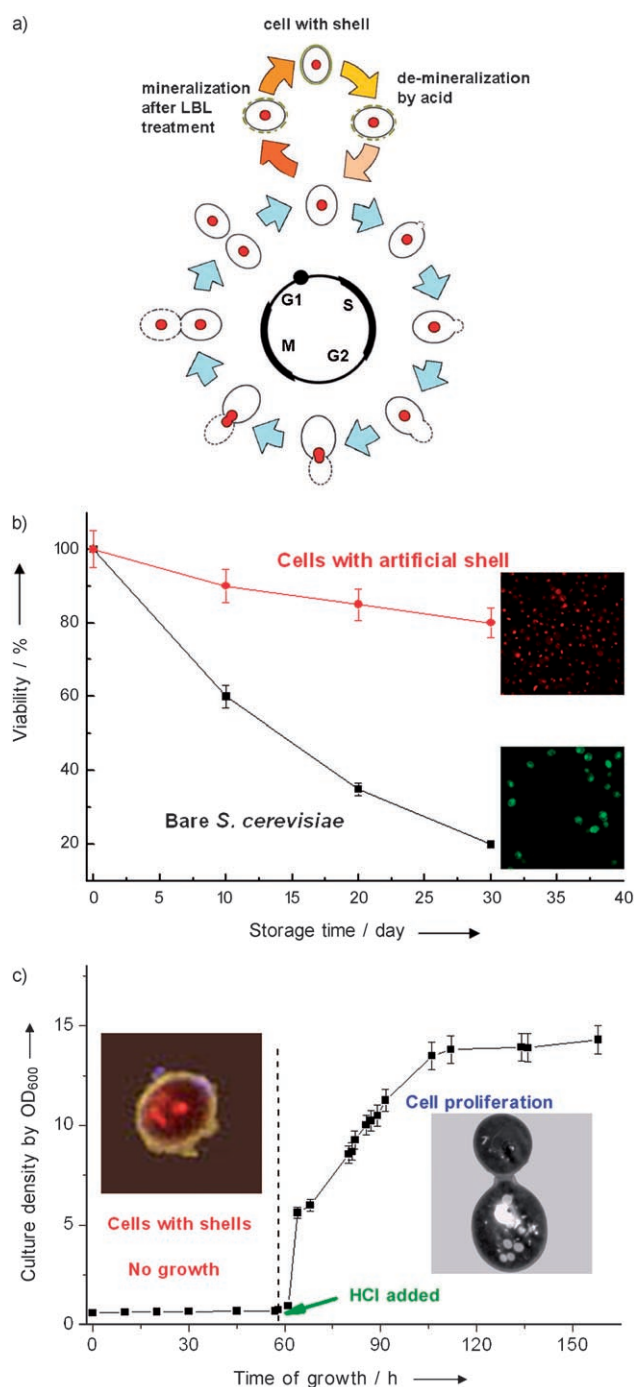
Figure 3. a) The lifecycle of normal yeast cells and the encapsulated cells. b) Curves showing the percentage of living cells in pure water against time. The inserts are the corresponding fluorescent images after 30 days obtained by using the live–dead viability probe FUN 1. The red spots imply that the cells are still alive, and green spots represent the dead cells. c) Growth curve of *S. cerevisiae* cells with and without the mineral shells. The culture density is measured by turbidity (OD$_{600}$). The cells with shells in this experiment were collected at the end of the cell survival test (Figure 4) so that all the living cells are perfectly encapsulated. 1 mM HCl was added at $t = 60$ h to induce the dissolution of the mineral shell. Left insert: fluorescent image confirming that the cells are alive; right insert: TEM image showing a dividing cell in the culture.

dividing resting state, known as the stationary phase or G0, and become inert.[24] *S. cerevisiae* enters into G0 state when it is encapsulated by the mineral since proliferation of the encased cells is not observed even in the nutritive medium. At a temperature of 4 °C, bare *S. cerevisiae* cells also become inert in pure water owing to the lack of nutrients. However, most of the bare cells ($> 80\%$) die in water within one month, indicating their short life. Coated by the calcium artificial shells, most encapsulated cells ($\approx 85\%$) are still alive in water even after one month (Figure 3b). The death of cells with shells, another $\approx 15\%$, may be caused by the original defects on the shells (indicated by arrows in Figure 1e). These experimental findings imply that the mineral shell prolongs life of the well-enclosed cell. It is reasonable to assume that the calcium phosphate shell can reduce mass transport and biological communication between the cells and its environment. The calcium phosphate layers are penetrated by oxygen and some small nutrients (such as H_2O), analogous to the function of eggshells.[25] However, their diffusion and transport through the mineral layers is slow, and a new molecular gradient is established,[26] which switches the cell to the inert state. Since the lifetime of the encapsulated cell is also extended, this technique can be used for cell storage.

The inert *S. cerevisiae* cells can be reactivated (G1 phase) by dissolving the mineral shell. Figure 3c shows that the well-enclosed cells remain in the resting state (G0) in a glucose-based media (YPD) at temperature of 30 °C and that there is no proliferation. In contrast, the proliferation of bare *S. cerevisiae* cells can be observed under the same experimental conditions. However, growth of the encapsulated *S. cerevisiae* cells is induced when the artificial shells are removed. In the experiment, the calcium phosphate mineral shell disappears upon spontaneous demineralization in a slightly acidic media (pH 5.5), which is caused by addition of HCl solution. It should be mentioned that yeast are viable over a relatively wide pH range of 3–8.[27] The released *S. cerevisiae* cells can grow and spontaneously switch to the cycling mode (Figure 3c) in the YPD media. The reactivated cells can be cultured like the normal *S. cerevisiae* cells, and they undergo DNA synthesis (S phase), the G2 phase, and mitosis (M phase). Dividing *S. cerevisiae* cells are also detected (insert in Figure 3c) by TEM. It is noted that the proliferation curve of the reactivated cells is exactly same as that of the ordinary *S. cerevisiae* cells,[24] implying that the biological functions and activity of living cells are not affected by the encapsulation and reactivation cycle (Figure 3a). Recently, we have also reported that the breakdown of hollow calcium phosphate shells can be precisely controlled by ultrasonic treatments;[28] this would provides another pathway to reactivate therapeutic cells in human body.

The artificial shell also serves as an enhanced safeguard to protect the living cells against foreign aggression. The encased cells can even live under hostile conditions. A lytic enzyme mixture can digest the cell wall that protects *S. cerevisiae* from rupture by osmotic stress. Zymolyase contains both a protease with affinity for mannoproteins and β-1,3-glucanase, which releases pentasaccharides from pachyman or laminarin.[29] The actions of both enzymes are required to lyse yeast cells. The course of lysis can be followed as a function of the

decrease in light scattering in a spectrophotometer. Normal bare yeast cells and the cells with LbL coatings cannot survive in a hypotonic solution in the presence of zymolyase. The cells cannot maintain homeostasis, and they burst without the cell walls. However, the artificial mineral shell can maintain the wall integrity by preventing the enclosed cells from contact with the external zymolyase. Although outer layer of the calcium shell is porous, the thick inner part can block the penetration of relatively large zymolyase (dimensions of β-1,3-glucanase $8.7 \times 8.7 \times 15.6$ nm^3)[30] since does not provide the convenient tunnels. Furthermore, calcium phosphates can strongly adsorb biological compounds such as proteins. Thus, the movement of zymolyase from the solution towards the cell is suspended. Figure 4 shows that in the presence of zymo-
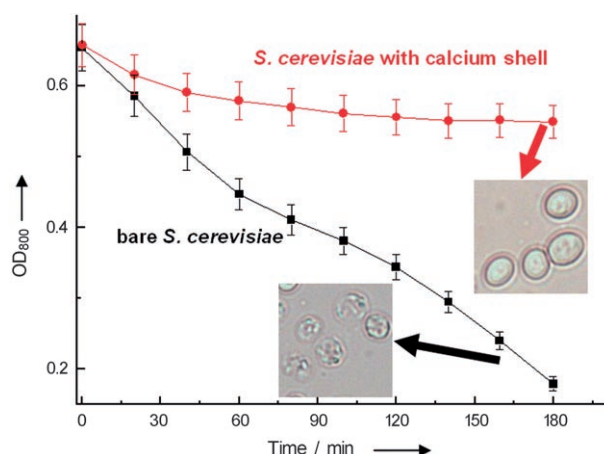
Figure 4. Survival of *S. cerevisiae* cells in the presence of zymolyase. Lysis was measured spectrophotometrically in a hypotonic solution in the present of zymolyase. The optical density of the cell suspension decreases as the cells lyse. The two inserts are the corresponding optical photos of the cells at the end of the experiments. It can be seen that zymolyase digests the cell wall and the cells cannot maintain homeostasis and burst without the protection of the mineral shells.

lyase, about 80% of the bare cells die within 3 h. However, most of the encapsulated *S. cerevisiae* cells ($\approx 85\%$) are still alive in such a hostile solution. Clearly, the artificial mineral shells show improved protection, and the encapsulated cells can even resist this natural toxin. Interestingly, the percentage of the surviving cells in this experiment is $\approx 85\%$, which is the same survival rate as in the lifetime test in pure water. Here, too, the death of the cells may be attributed to defects in the shells, by which zymolyase can still reach the cells. It implies that the percentage of the "perfect" shells prepared by this method is about 85%. Since the size of the transport tunnel is an important control factor, the porosity and the thickness of the calcium shell can be adjusted to achieve different protection effects; this was also confirmed experimentally (see Figures S2 and S3 in the Supporting Information). In addition, atomic force microscopy (AFM) studies show that the mechanical strength of the mineralized cells is also improved significantly by the shell (see Figure S4 in the Supporting Information).

The shells can also be used as scaffolds for the chemical and biological regulation of the living cells; this implies further applications of the shells in cell identification and regulation. Here, we show that *S. cerevisiae* cells become magnetic by modification of the mineral shells. Fe$_3$O$_4$ nanocrystals can be incorporated into the mineral shell during the precipitation of calcium phosphate. With a complex shell of calcium phosphate and Fe$_3$O$_4$, the encapsulated cells can be driven by a magnetic force and they can be concentrated quickly around a magnet (Figure 5 and Figure S5 in the
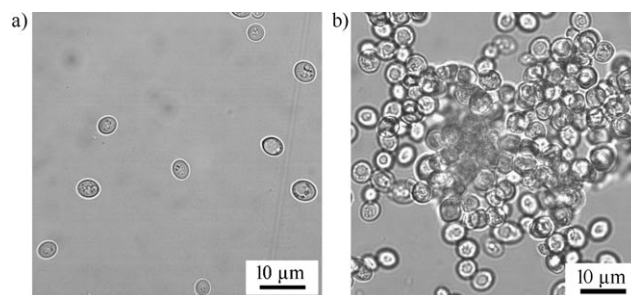
Figure 5. *S. cerevisiae* cells become magnetic by incorporation of Fe$_3$O$_4$ into the shells. a) Cells are randomly distributed in solution. b) Cells are attracted by a magnetic field and they gather around a magnet placed under the substrate (marked by the dashed circle). Since the magnet is relatively small, some cells were packed perpendicular to the substrate, resulting in the blurry image.

Supporting Information). Since synthesis of shells can be controlled easily in laboratory, biological modification through this artificial layer becomes convenient and effective. We suggest that cells with functional shells can be prepared by incorporation of proteins into well-designed mineral structures in future.

By a combination of the functions of storage, protection, and chemical modification, the artificial mineral shell can be an ideal vehicle for living cells. In cell engineering and therapy, the cells with a longer storage time are always preferred, and living cells are frequently required to pass through a hostile milieu to reach the desired sites. These problems can be solved by using the artificial shell. Currently modification of the biological behavior of living cells is of interest for a variety of technological objectives. In this context biomimetic mineralization may provide an inexpensive but effective strategy.

Experimental Section

Biomimetic mineralization: *S. cerevisiae* cells, strain AS2.440, were grown in YPD medium (2% peptone, 1% yeast extract, and 2% glucose) incubated at 30°C with shaking at 220 rpm. Cells were collected by centrifugation and washed with 0.12 M NaCl. Typical adsorption conditions used to form the polyelectrolyte layers on the cells: 1 g L^{-1} of poly(diallyldimethylammonium chloride) (PDADMAC, $M_w = 10000$–20000 Da) and poly(acrylic sodium) (PAA, $M_w = 5100$ Da) in 0.12 M NaCl. The cell concentration was 10^7 cells per mL. The eight-layer, (PDADMAC/PAA)$_4$, polyelectrolyte-coated cell was obtained by LbL treatment (see the Supporting Information). To prepare the shell of calcium phosphate, 10 mL of a mixture, which

contained the cells after the LbL treatment (10^7 cells per mL) and 10 mM $CaCl_2$, was stirred and titrated with 10 mL Na_2HPO_4 (10 mM) at a rate of 1 mL min^{-1}; the pH of the reaction solution was maintained at 6.8 using 0.01 M NaOH; the reaction time was 1 h. Bare cells were used in the control experiment. The obtained cell samples and the bare *S. cerevisiae* cells were stored in a YPD media at 4 °C

Magnetic modification: Fe_3O_4 particles (9.0 ± 1.2 nm) were added to the mixture of LbL-treated cells and $CaCl_2$. The concentration of Fe_3O_4 was 1.25 g L^{-1}. All the other experimental processes were the same as the above. A drop of the obtained cell solution (10^7 cells per mL) was applied to a glass slide and the cells were observed under an optical microscope (Nikon, Japan). A magnetized needle (tip size ≈ 20 μm) was put under the slide to induce the aggregation of the cells around the magnet, which was driven by the interaction of Fe_3O_4 and the magnetic field.

Characterization: SEM and TEM studies were conducted with JSM-35CF (JEOL, Japan) and JEM-200CX (JEOL, Japan), respectively. The cells were washed using PBS solution and distilled water. They were lyophilized with Vertris 12SL (Vertris, USA). Biological TEM was performed using JEM-1200EX (JEOL, Japan). The specimens were fixed with gluteraldehyde, OsO_4, and $K_2Cr_2O_7$, and were dehydrated in ethanol/acetone. They were embedded in Epon 812/Araldite M resin. Thin sections (80 ± 10 nm) were cut by using a Reichert ultratome (Zeiss, Germany) and were stained with uranyl acetate and lead citrate.

Fluorescence study: Molecular Probes' LIVE/DEAD Yeast Viability Kit (L-7009, Molecular Probes, USA) combined a two-color probe for yeast viability, FUN1, with a fluorescent fungal-surface-labeling reagent of a third color, Calcofluor White M2R (see http://probes.invitrogen.com). Tetracycline hydrochloride could coordinate with calcium ions to induce a golden-yellow fluorescence under UV light (360–370 nm), and it was used as a fluorescence probe for the calcium phosphate shell (its concentration in the media was 5 × 10^{-2} g L^{-1}). Images were acquired using a Zeiss LSM-510 confocal laser scanning microscope.

Lifetime test: The media was pure water since yeast could be stored in YPD at 4 °C for a long time period. The encapsulated and bare *S. cerevisiae* cells were suspended in the distilled water (concentration of 10^7–10^8 cells per mL) at 4 °C, and the cell samples were withdrawn periodically to test their viabilities.

Cell survival test: Zymolyase was the principal enzyme source used for the survival test. Lyophilized enzyme was dissolved in water to a concentration of 1.5 g L^{-1}. Cells were collected by centrifugation and were washed with distilled water. Then they were suspended in medium consisting of 0.1 M Tris-SO_4, 10 mM 1,4-dithiolthreitol (DTT), pH 9.4 and incubated at 30 °C for 10 min. After washing with 1.2 M sorbitol solution, the yeast cells were resuspended in 1.2 M sorbitol, 20 mM KH_2PO_4, pH 7.2. Yeast cells were treated with zymolyase (341 U mg^{-1}) and incubated at 30 °C. The formation of the spheroplasts was minotored by reading the OD_{800} of the sample.

[1] H. A. Lowenstam, S. Weiner, *On Biomineralization*, Oxford University Press, Oxford, **1989**.

[2] S. Mann, J. Webb, R. J. P. Williams, *Biomineralization: Chemical and Biochemical Perspectives*, VCH, New York, **1989**.

[3] S. Weiner, H. D. Wagner, *Annu. Rev. Mater. Sci.* **1998**, *28*, 271–298.

[4] R. R. Naik, M. O. Stone, *Mater. Today* **2005**, *8*, 18–26.

[5] M. Sarikaya, *Proc. Natl. Acad. Sci. USA* **1999**, *96*, 14183–14185.

[6] C. E. Hamm, R. Merkel, O. Springer, P. Jurkojc, C. Maier, K. Prechtel, V. Smetacek, *Nature* **2003**, *421*, 841–843.

[7] J. C. Mell, S. M. Burgess, *Encycl. Life Sci.* **2002**, 1–8.

[8] D. Botstein, G. R. Fink, *Science* **1988**, *240*, 1439–1443.

[9] A. Goffeau, B. G. Barrell, H. Bussey, R. W. Davis, B. Dujon, H. Feldmann, F. Galibert, J. D. Hoheisel, C. Jacq, M. Johnston, E. J. Louis, H. W. Mewes, Y. Murakami, P. Philippsen, H. Tettelin, S. G. Oliver, *Science* **1996**, *274*, 546–567.

[10] E. Cabib, D. H. Roh, M. Schmidt, L. B. Crotti, A. Varma, *J. Biol. Chem.* **2001**, *276*, 19679–19682.

[11] S. Mann, *Nature* **1988**, *332*, 119–124.

[12] S. Mann, D. D. Archibald, J. M. Didymus, T. Douglas, B. R. Heywood, F. C. Meldrum, N. J. Reeves, *Science* **1993**, *261*, 1286–1292.

[13] L. Addadi, S. Weiner, *Proc. Natl. Acad. Sci. USA* **1985**, *82*, 4110–4114.

[14] L. Addadi, J. Moradian, E. Shay, N. G. Maroudas, S. Weiner, *Proc. Natl. Acad. Sci. USA* **1987**, *84*, 2732–2736.

[15] K. Bronsch, T. Diamantstein, *Nature* **1965**, *207*, 635–636.

[16] M. Soledad Fernandez, A. Moya, L. Lopez, J. L. Arias, *Matrix Biol.* **2001**, *19*, 793–803.

[17] a) G. Decher, J. D. Hong, J. Schmitt, *Thin Solid Films* **1992**, *210*, 831–835; b) G. Decher, *Science* **1997**, *277*, 1232–1237; c) E. Donath, G. B. Sukhorukov, F. Caruso, S. A. Davis, H. Möhwald, *Angew. Chem.* **1998**, *110*, 2323–2327; *Angew. Chem. Int. Ed.* **1998**, *37*, 2201–2205.

[18] L. Richert, P. Lavalle, E. Payan, X. Z. Shu, G. D. Prestwich, J. Stoltz, P. Schaaf, J. Voegel, C. Picart, *Langmuir* **2004**, *20*, 448–458.

[19] P. A. Ngankam, P. Lavalle, J. C. Voegel, L. Szyk, G. Decher, P. Schaaf, F. J. G. Cuisinier, *J. Am. Chem. Soc.* **2000**, *122*, 8998–9005.

[20] a) D. G. Shchukin, G. B. Sukhorukov, H. Möhwald, *Chem. Mater.* **2003**, *15*, 3947–3950; b) A. Antipov, D. Shchukin, Y. Fedutik, I. Zanaveskina, V. Klechkovskaya, G. B. Sukhorukov, H. Möhwald, *Macromol. Rapid Commun.* **2003**, *24*, 274–277; c) D. G. Shchukin, G. B. Sukhorukov, H. Möhwald, *Angew. Chem.* **2003**, *115*, 4610–4613; *Angew. Chem. Int. Ed.* **2003**, *42*, 4472–4475; d) D. G. Shchukin, G. B. Sukhorukov, *Adv. Mater.* **2004**, *16*, 671–682.

[21] N. A. J. M. Sommerdijk, E. N. M. van Leeuwen, M. R. J. Vos, J. A. Jansen, *CrystEngComm* **2007**, *9*, 1209–1214.

[22] M. Chanana, A. Gliozzi, A. Diaspro, I. Chodnevskaja, S. Huewel, V. Moskalenko, K. Ulrichs, H. J. Galla, S. Krol, *Nano Lett.* **2005**, *5*, 2605–2612.

[23] A. Diaspro, D. Silvano, S. Krol, O. Cavalleri, A. Gliozzi, *Langmuir* **2002**, *18*, 5047–5050.

[24] a) M. Werner-Washburne, E. Braun, G. C. Johnston, R. A. Singer, *Microbiol. Rev.* **1993**, *57*, 383–401; b) P. K. Herman, *Curr. Opin. Microbiol.* **2002**, *5*, 602–607.

[25] A. L. Romanoff, *Biol. Bull.* **1929**, *56*, 351–356.

[26] S. G. Zhang, *Nat. Biotechnol.* **2004**, *22*, 151–152.

[27] T. Imai, T. Ohno, *Appl. Environ. Microbiol.* **1995**, *61*, 3604–3608.

[28] Y. Cai, H. Pan, X. Xu, Q. Hu, L. Li, R. Tang, *Chem. Mater.* **2007**, *19*, 3081–3083.

[29] K. Kitamura, T. Kaneko, Y. Yamamoto, *Arch. Biochem. Biophys.* **1971**, *145*, 402–404.

[30] J. N. Varghese, T. P. J. Garrett, P. M. Colman, L. Chen, P. B. Hoj, G. B. Fincher, *Proc. Natl. Acad. Sci. USA* **1994**, *91*, 2785–2789.